OPEN ACCESS

Nano Biomed Eng

ISSN 2150-5578 http://nanobe.org

Review

Hydrothermal/Solvothermal Synthesis of Graphene Quantum Dots and Their Biological Applications

Minghan Xu, Zhaohui Li, Xingzhong Zhu, Nantao Hu, Hao Wei, Zhi Yang*, Yafei Zhang*

Key Laboratory for Thin Film and Microfabrication of Ministry of Education, Research Institute of Micro/Nano Science and Technology, Shanghai Jiao Tong University, Shanghai 200240, P. R. China.

*Corresponding authors: zhiyang@sjtu.edu.cn (Zhi Yang); yfzhang@sjtu.edu.cn (Yafei Zhang)

Abstract

Graphene quantum dots (GQDs), as a new class of zero dimensional fluorescent carbon material, have been used in physical, chemical and biological aspects for many interesting properties, such as low toxicity, excellent solubility, high chemical stability, and good surface activity. As a green synthetic method, hydrothermal/solvothermal technology has been applied to effectively control characteristics of GQDs. In this review, we summarize recent work on the hydrothermal/solvothermal synthesis of GQDs and their emerging biological applications.

Keywords: Graphene quantum dots, Hydrothermal, Solvothermal, Biological applications

Citation: M.H. Xu et al. Hydrothermal/Solvothermal Synthesis of Graphene Quantum Dots and Their Biological Applications. Nano Biomed. Eng. 2013, 5(2), 65-71.
DOI: 10.5101/nbe.v4i3.p65-71.

1. Introduction

Graphene quantum dots (GQDs), as sp^2-hybrid single layer nanocrystals, are highly fluorescent in solution or/and film state, even in live cells, due to their quantum confinement and edge effects. The synthetic methods of GQDs mainly include two categories, top-down and bottom-up. Top-down method is based on sp^2-hybridized carbon materials, such as graphene oxide, carbon fiber, and carbon nanotube, treated with mixed acids [1,2] or by electrochemical methods [3] to cut them into small pieces. Bottom-up method is based on small molecules like glucose [4,5] and citric acid [6] to assemble, polymerize and carbonize to nanoscale product. As shown in Fig. 1, more and more publications have emerged on GQDs, not only in the synthesis of GQDs, but also in their implementation in photovoltaic devices, fuel cells, light-emitting diodes, and bioimaging.

Among many synthetic methods of GQDs, the hydrothermal/solvothermal (H/S) synthesis is the most used one. H/S synthesis is an important technology to produce most inorganic materials. H/S synthesis provides a sealed autoclave environment to form high pressure and high temperature to obtain good crystal morphology. Many carbon allotropes, such as carbon nanotube, nanodiamond, carbon dot, carbon sphere, and carbon aerosol, have been sophisticated synthesized by H/S reaction. Recent advances on H/S synthetic technologies of GQDs were summarized in Table 1.

2. H/S synthesis

Hydrothermal synthesis has a strong influence on the formation and particle size of GQDs. Water, as a green solvent used in hydrothermal synthesis, plays an important role in atom-economical reactions. D. Pan et al. [7] for the first time applied hydrothermal technology to synthesize GQDs. Firstly, graphene sheets obtained by thermal treatment of graphene oxide sheets were cut by mixed acids under mild ultrasonication. Subsquently the treated suspension was transferred to Teflon-lined autoclave to get small GQDs mainly distributed between 5 to 13 nm (average diameter: 9.6 nm). As seen in Fig. 2, the reaction mechanism was proposed to be that epoxy groups and carbonyl groups in the graphene sheets structure were easily fragile and attacked during the hydrothermal deoxidization process. Later, they further modified their method by high-temperature thermally-treated graphene sheets on the strong alkaline condition to prepare well-crystallized GQDs [8].

Graphene has attracted tremendous interest in electronics, solar cell, Li-ion battery, and pollution treatment. The modification of graphene, such as N-doping and

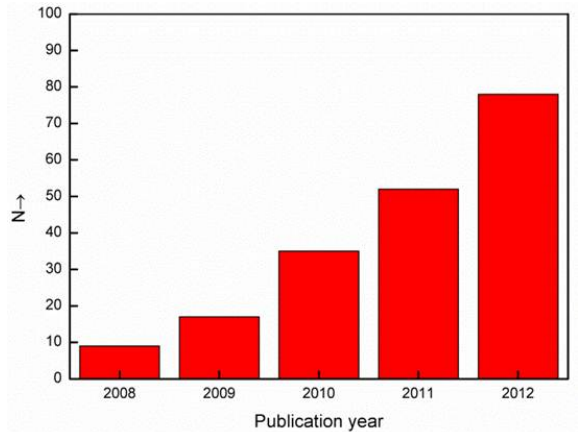

Fig. 1 The increase in the number of publications about graphene quantum dots based on Web of Science database.

B-doping, may alter its electric properties. Based on the same doping treatment, photoluminescence and electric properties of doped GQDs may be adjusted by changing their band gap. H. Tetsuka et al. [9] reported extraction of amine-functionalized graphene quantum dots (NH_2-GQDs) using oxidized graphene sheets and ammonia in hydrothermal condition by bond-scission reaction. Photoluminescence color from violet to yellow could be changed by controlling the concentration of ammonia and the hydrothermal temperature. As shown in Fig. 3, nucleophilic substitution is taken place to react with epoxide group to get sp^2 domains with ammonia electron-pair's attacking. Whether the reaction temperature was changed or not, the size of GQDs was about 2.7 nm according to Raman spectrum and TEM image.

Y. Liu et al. [10] implemented PAN-based carbon fiber to get 35 nm N-GQDs and then controlled the hydrothermal time in ammonia solution to get 3 nm N-GQDs on the bond-scission strategy using ammonia as a passivation agent. The strategy for synthesis of N-GQDs was illustrated in Fig. 4. Similar work could also be seen in ref. [11] and [12].

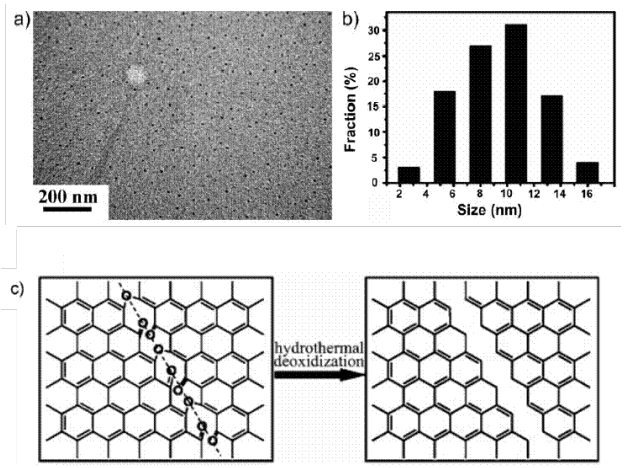

Fig. 2 a) TEM image of GQDs. b) Diameter distribution of GQDs. c) Mechanism for hydrothermal deoxidization of oxidized graphene sheets into GQDs. Copyright permission from ref. [7].

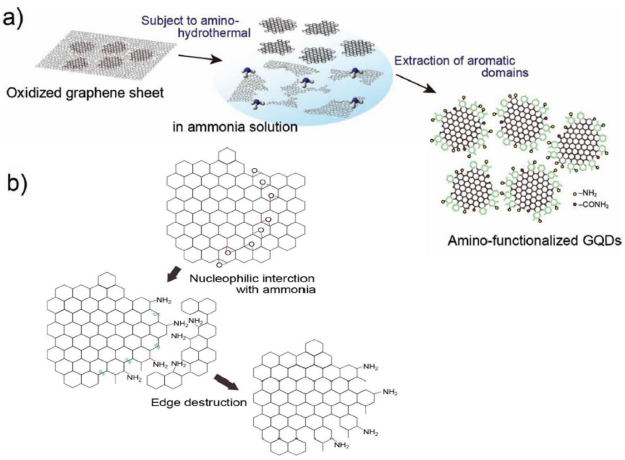

Fig. 3 a) Schematic illustration of the preparative strategy for NH_2-GQDs. b) Schematic illustration of the proposed formation mechanism for NH_2-GQDs. Copyright permission from ref. [9].

Table 1 A summary of the characteristics of GQDs synthesized via H/S methods.

Methods	Materials	Size (nm)	Height (nm)	Color	Temperature/Time (ºC/h)	Ref.
Hydrothermal	OGSs, NaOH	5-13	1-2	blue	200/10	7
Hydrothermal	OGSs, ammonia	1.5-5	1.5-1.9	green	200/10-12	8
Hydrothermal	OGSs, ammonia	2.5	1.13	violet to yellow	70-150/5	9
Hydrothermal	N-GQDs, ammonia	ca.3	1.3-3	yellow to cyan	200/1-14	10
Hydrothermal	GO, ammonia	2-6	0.5-3	blue	180/12	11
Hydrothermal	GO, ammonia	2.5-4.5	3-5	blue	200/2-8	12
Hydrothermal	FG	1-7	—	blue	200/10	13
Hydrothermal	ONG	1-7	—	blue	180/10	14
Hydrothermal	Cutting GO, PEG10000	5-25	—	blue	200/24	15
Hydrothermal	Ozonized RGO	2-5	—	blue	200/10	16
Microwave-Hydrothermal	Glucose	1.65-21	3.2	DUV, blue	—/1-11	4
Microwave-Hydrothermal	Glucose, PEG20000	1.5-3.9	1.8, 2.3, 2.5	blue	—/1-9	5
Microwave-Hydrothermal	GO, mixed acids	ca.3	< 0.7	blue	200/5	17
Solvothermal	GO, DMF	5.3	1.2	green	200/5	18
Solvothermal	GO, DMF	3-5	0.95	blue to green	200/8	19
Solvothermal	GO, DMF	3	0.5-1	green	200/4.5	20

[a]: "—" stands for no information.

[b]: OGSs: Oxidized graphene sheets, N-GQDs: Nitrogen doped GQDs, GO:Graphene oxide, FG: Fluorinated graphene, ONG: Oxidized N-doped graphene, RGO: Reduced graphene oxide, DUV: Deep ultraviolet.

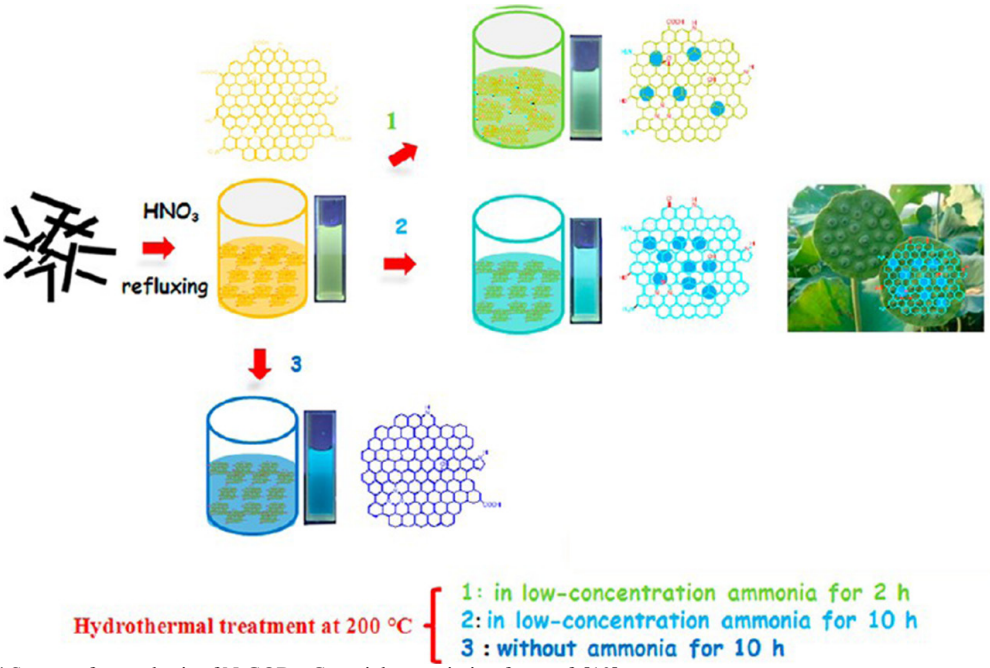

Fig. 4 Strategy for synthesis of N-GQDs. Copyright permission from ref. [10]

Q. Feng et al. [13] demonstrated that fluorinated graphene could be obtained by high temperature treatment with reduced graphene oxide and XeF_2, strong acid oxidizing, and finally hydrothermal reaction to obtain fluorinated GQDs (F-GQDs). F-GQDs showed a red-shift by 10 nm compared with undoped GQDs and had an obvious up-conversion photoluminescence that might be used as an effective photocatalyst. Functionalized with small molecules and polymers [5,15], GQDs will tune their luminescence and enhance their biocompatibility.

Microwave-hydrothermal (MH) method is an integrated technology of microwave field and hydrothermal method. Compared with traditional hydrothermal method, MH method can accelerate the kinetics of reaction, shorten the reaction time, and form novel phases. L. Tang et al. [4] used glucose, sucrose, and fructose as carbon source to synthesize water soluble GQDs in a short time under different powers. The obtained GQDs exhibited deep UV emission and had approximately 3.5 nm diameter. As seen in Fig. 5, the reaction mechanism was that glucose molecules were dehydrated to form the core and then edge grew with increasing microwave heating time. Owing to the closed system, the precursor was arranged to crystalline GQDs.

Recently, L. Tang et al. [5] modified glucose based on MH method using PEG 20000 as soft template and glucose as carbon source. The reaction process went through carbonizing, nucleating, crystallizing, and growing up to finally obtain narrow-size distribution GQDs. S. Chen et al. [17] reported graphene oxide aqueous solution treated with mixed acids in MH method could acquire GQDs. As shown in Fig. 6, in strong acid solution and high concentration, GQDs showed self-assembled J-type aggregation.

Solvothermal reaction is a type of synthetic method using organic solvents (benzene, DMF or DMSO), instead of water to obtain desired reaction products. Because the organic solvents have an important effect on the size and morphology of products, it is necessary to check the chemical nature and physicochemical properties of the solvents. S. Zhu et al. [18] used DMF as a solvent and weak reduction agent to split graphene oxide into the fluorescent green GQDs. The GQDs were obtained by column chromatography on silica gel instead of dialysis treatment. Later on, they increased the reaction time to 8 h, used methanol/methylene chloride and water as

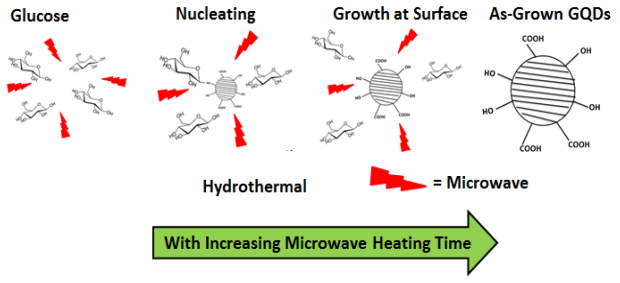

Fig. 5 Preparation mechanism of GQDs by MH method.

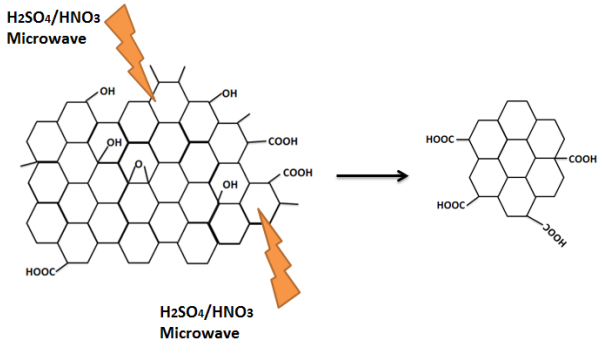

Fig. 6 Oxidation cutting of graphene oxide into GQDs by mixed acids.

mobile phase to get GQDs [19]. It was interesting that the obtained GQDs had the same size and height but different fluorescent absorption peaks. Their fluorescence mechanism was attributed to energy traps.

3. Biological Applications

3.1 Cell/Tissue imaging

GQDs have more advantages for cell imaging due to their low cytotoxicity, good biocompatibility and excellent photostability. The recent work was summarized in Table 2.

J. Peng et al. [26] evaluated the cytotoxicity of two kinds of GQDs with green and blue fluorescence by using two different human breast cancer cell lines MDA-MB-321 and T47D with MTT viability assay. These GQDs didn't impose obvious cytotoxicity the same as those in other work [18,24]. As shown in Fig. 7, images visualized the phase contrast image of T47D cells, the nucleus stained blue with DAPI, agglomerated green GQDs around each nucleus and overlay image of cell with phase contract, DAPI and green GQDs.

Y. Dong et al. [1] performed MCF-6 cells as bio-imaging cells exhibiting a bright green color when imaged on the confocal laser scanning microscope. GQDs labeled not only cell membrane and the cytoplasm, but also the nucleus. This was the first time for using photoluminescence carbon nanostructures to label the cell nucleus. L. Deng et al. [29] used hybrid Au NCs@SiO_2@GQDs nano-composites binding with anti-EGFR (epidermal growth factor receptor) to selectively image cell membrane.

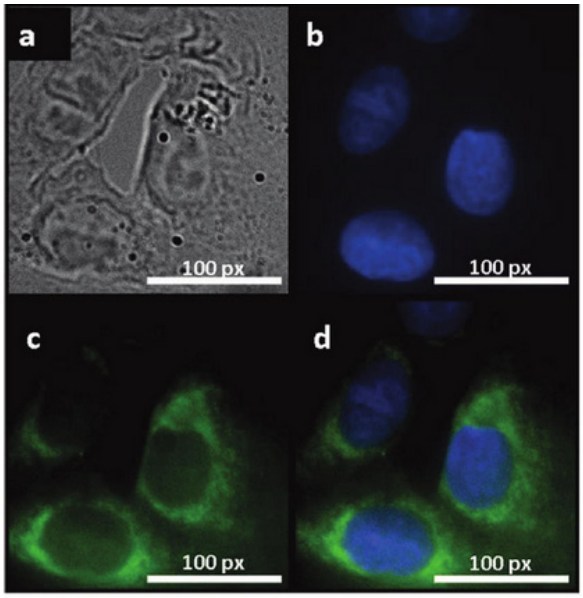

Fig. 7 Fluorescent images of human breast cancer cell T47D after incubation with green GQDs for 4 h (a) phase contrast picture of T47D cells. (b) Individual nucleus stained blue with DAPI. (c) Agglomerated green GQDs surrounding each nucleus. (d) The overlay high contrast image of nucleolus stained with blue DAPI and GQDs (green) staining. Copyright permission from ref. [26].

Up-conversion photoluminescence is less harmful to living cells or biosystems than one-photon UV or blue excitations. S. Zhu et al. [22] reported up-conversion photoluminescence of GQDs exploring in cell imaging. As shown in Fig. 8, it was found that bright green or blue area inside MC3T3 cells labelled under near infra-red excitation (808 nm), indicating successful translocation of GQDs through cell membrane.

Table 2 Summary of recent works on cell imaging of GQDs methods.

Excitation Wavelength (nm)	GQDs Concentration	Cells Concentration	Imaging Cells	Imaging Position	Color	Ref.
405, 488, (405)	2.5 mg/mL	10^4 cells/150 μL	MG-63 (MC3T3)	Cell cytoplasm. (Cell[a])	green yellow (green)	18
405	25 μg/mL	3×10^5 cells/well	A549 MCF-7	Cell cytoplasm	yellow	21
808	2.5 mg/mL	10^4 cells/150 μL	MC3T3	Cell cytoplasm	bright green or blue	22
488	200 μg/mL	1×10^5 cells/well	U251	Cell	green	23
405	0.01 mg/mL	1×10^5 cells/ml	HeLa	Cell nucleus	green	8
405	25 μg/mL	1-3×10^5 cells/well	NSCs, PPCs, CPCs (stem cell)	Cell cytoplasm	yellow	24
488	100 μg/mL	1×10^4 cells/cm^2	MCF-7	Cell membrane, cytoplasm, nucleus	green	1
405	—	—	HeLa	Cell cytoplasm	green	25
Nikon Intensilight C-HGFI lamp	50 μg/mL	1×10^4 cells/500 μL	T47D	Cell cytoplasm	green	26
380	100 μg/mL	1×10^4 cells/well	A549	Cell membrane, cytoplasm	blue	27
405	5, 10, 25, 50 or 100 μg/mL	1×10^5 cells/dish	A549	Cell cytoplasm	green or blue	28
405	0.1 mg/mL	5×10^4 cells/mL	HeLa	Cell cytoplasm	green	11
—[b]	0.05 nM[c]	—	HeLa	Cell membrane	yellow	29
—	0.1 mg/mL	5×10^4 cells/mL	MDA-MB231	Cell	red	30
800	50 μg/ mL	5×10^5 cells/mL	HeLa	Cell membrane, cytoplasm	green	20

[a]: Cell means whole cell image based on confocal laser scanning microscope.
[b]: "—"stands for no information.
[c]: Au NCs@SiO_2@GQDs nanocomposites, Au NCs: gold nanocubes.

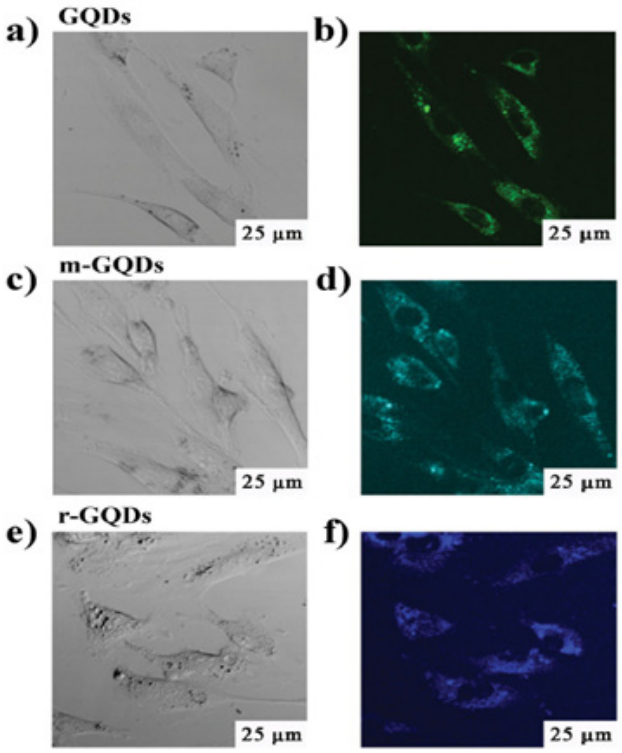

Fig. 8 The up-conversion cellular imaging of GQDs. The washed cells imaged under bright field (a, c, e) and 808 nm excitation (b, d, f). The detection wavelength was in the 490-550 nm range for GQDs, 450-500 nm for modification GQDs, and 420-460 nm for reducing GQDs. Copyright permission from ref. [22].

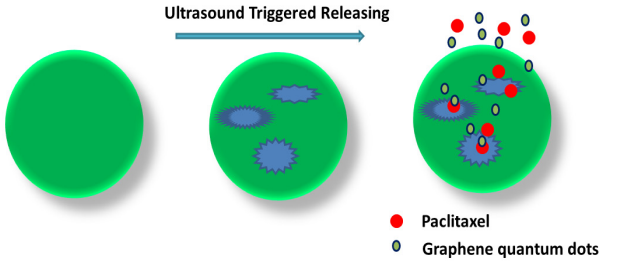

Fig. 9 Schematic illustration for procedures of shell cracking and drug release under ultrasound.

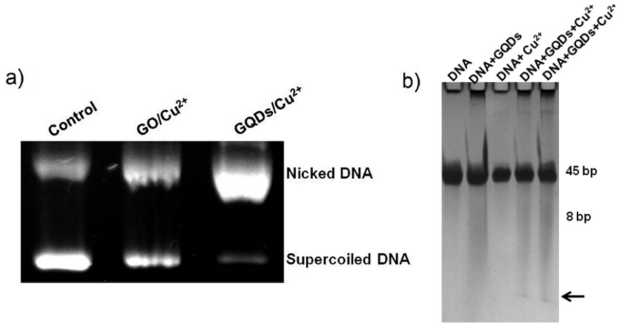

Fig. 10 a) Agarose gel electrophoresis of GO and GQDs with Cu^{2+} incubated for 2 h at 37 ºC in 50 mM Tris buffer (pH 7.2). Cu^{2+} was 10 mM, GO and GQDs were both 50 μg/mL. b) SDS-PAGE of a short DNA helix (45 bp) cleaved by GQDs and Cu^{2+}. The arrow indicated the small fragment. Copyright permission from ref. [36].

Although many separation technologies [31,32] and synthetic methods [33] have been reported on carbon dots, there are few work on synthesis of long-wavelength and multicolor GQDs. Recently, M. Nurunnabi et al. [30] reported treating carbon fibers in mixed acids and citric acid to obtain near infra-red GQDs by controlling the ratio of mixed acids and the reaction temperature. They performed these particles to image cells, even nude mice. GQDs as a noninvasive imaging agent can be detected at the heart, liver, spleen and kidney at 8 h post injection.

Recently, two-photon deep-tissue imaging was demonstrated by Q. Liu et al. [20]. N-GQDs could achieve a large depth of 1800 μm, which extended the fundamental imaging depth limit of two-photon microscopy.

3.2 Drug delivery

GQDs had been applied to drug delivery combined with targeted drug by weak interaction reported by X. Sun et al. [34]. Y. Jing et al. [35] reported a multifunctional capsule platform for simultaneous fluorescence imaging, magnetically guided delivery, and ultrasound-triggered releasing, which was fabricated by two coaxial electrospray immiscible liquids. As a tracer for capsule targeting and a marker for drug releasing, the role of GQDs was luminescence imaging (Fig. 9).

3.3 DNA intercalator

The choice of DNA cleavage is of importance for understanding the mechanism of DNA scission, repair, and signal transduction. X. Zhou et al. [36] reported that using GQDs/Cu^{2+} as a DNA intercalator was better than using GO/Cu^{2+} which they previously worked [37]. While 59% supercoiled DNA was cleaved by using GO/Cu^{2+}, 90% supercoiled DNA was converted into nicked DNA by using GQDs/Cu^{2+}. As seen in Fig. 10, when a short DNA helix (45 bp) was used, GQDs/Cu^{2+} could cut short duplex into small fragments. While in other control experiment, no small pieces was observed.

3.4 Other biological applications

Z.M. Markovic et al. [23] reported that GQDs produced by electrochemical methods showed morphological and biochemical characteristics of both autophagy and apoptosis owing to generating reactive oxygen species when irradiated. It was potential that GQDs could be used as an autophagy-inducing photodynamic agent. X. Chen et al. [38] used GQDs to stabilize i-motif structures under acidic conditions. In addition, under alkaline or physiological conditions, GQDs could promote the formation of i-motif structures. H. Zhao et al. [39] provided a novel signal transduction strategy between graphene and GQDs for the sensitive detection of human immunoglobulin G (InG) based on fluorescence resonance energy transfer (FRET). Glutathione-functionalized GQDs could be used to estimate ATP level in cell lysates and human blood serum as selective fluorescence probes [40]. F. Jiang et al. [41] reported that NH_2-GQDs as a anticoplasma agent protected cells from infection due to their peroxidase catalytic activity.

4. Conclusions

Using the hydrothermal, microwave-hydrothermal and solvothermal technology, GQDs can be synthesized with different sizes and tunable fluorescence. With the deep research on GQDs, different methods and techno-logies may grow up and enlarge the reserch scope. Due to low toxicity and high fluorescence, GQDs have been used in cell imaging, drug delivery, DNA intercalator, and so on. It is believed that more novel biological applications will emerge in the near future.

Acknowledge

This work was supported by the National High-Tech R & D Program of China (863 program, 2011AA050504), National Natural Science Foundation of China (61006002 and 51102164), Program for New Century Excellent Talents in University (NCET-12-0356), Shanghai Science and Technology Grant (12JC1405700), Shanghai Pujiang Program (no. 11PJD011), the Program for Professor of Special Appointment (Eastern Scholar) at Shanghai Institutions of Higher Learning, Medical-Engineering Crossover Fund (YG2012MS40 and YG2012MS37) of Shanghai Jiao Tong University. We also acknowledge the analysis support from the Instrumental Analysis Center of Shanghai Jiao Tong University.

References

1 Y.Q. Dong, C.Q. Chen, X.T. Zheng, L.L. Gao, Z.M. Cui, H.B. Yang, C.X. Guo, Y.W. Chi, C.M. Li. One-step and high yield simultaneous preparation of single- and multi-layer graphene quantum dots from CX-72 carbon black. *J. Mater. Chem.*, 2012, 22: 8764-8766.

2 M.M. Xie, Y.S. Su, X.N. Lu, Y.Z. Zhang, Z. Yang, Y.F. Zhang. Blue and green photoluminescence graphene quantum dots synthesized from carbon fibers. *Mater. Lett.*, 2013, 93: 161-164.

3 D.B. Shinde, V.K. Pillai. Electrochemical preparation of luminescent graphene quantum dots from multiwalled carbon nanotubes. *Chem. Eur. J.*, 2012, 18: 12522-12528.

4 L.B. Tang, R.B. Ji, X.K. Cao, J.Y. Lin, H.X. Jiang, X.M. Li, K.S. Teng, C.M. Luk, S.J. Zeng, J.H. Hao, S.P. Lau. Deep ultraviolet photoluminescence of water-soluble self-passivated graphene quantum dots. *ACS Nano,* 2012, 6: 5102-5110.

5 L.B. Tang, R.B. Ji, X.M. Li, K.S. Teng, S.P. Lau. Size-dependent structural and optical characteristics of glucose-derived graphene quantum dots. *Part. Part. Syst. Charact.*, 2013, DOI: 10.1002/ppsc.201200131.

6 Y.Q. Dong, J.W. Shao, C.Q. Chen, H. Li, R.X. Wang, Y.W. Chi, X.M. Lin, G.N. Chen. Blue luminescent graphene quantum dots and graphene oxide prepared by tuning the carbonization degree of citric acid. *Carbon*, 2012, 50: 4738-4743.

7 D.Y. Pan, J.C. Zhang, Z. Li, M.H. Wu. Hydrothermal route for cutting graphene sheets into blue-luminescent graphene quantum dots. *Adv. Mater.*, 2010, 22: 734-738.

8 D.Y. Pan, L. Guo, J.C. Zhang, C. Xi, Q. Xue, H. Huang, J.H. Li, Z.W. Zhang, W.J. Yu, Z.W. Chen, Z. Li, M.H. Wu. Cutting sp^2 clusters in graphene sheets into colloidal graphene quantum dots with strong green fluorescence. *J. Mater. Chem.*, 2012, 22: 3314-3318.

9 H. Tetsuka, R. Asahi, A. Nagoya, K. Okamoto, I. Tajima, R. Ohta, A. Okamoto. Optically tunable amino-functionalized graphene quantum dots. *Adv. Mater.*, 2012, 24: 5333-5338.

10 Y. Liu, P.Y. Wu. Graphene quantum dot hybrids as efficient metal-free electrocatalyst for the oxygen reduction reaction. *ACS Appl. Mater. Interfaces*, 2013, 5: 3362-3369.

11 C.F. Hu, Y.L. Liu, Y.H. Yang, J.H. Cui, Z.R. Huang, Y.L. Wang, L.F. Yang, H.B. Wang, Y.Xiao, J.H. Rong. One-step preparation of nitrogen-doped graphene quantum dots from oxidized debris of graphene oxide. *J. Mater. Chem. B*, 2013, 1: 39-42.

12 Z.H. Zhang, P.Y. Wu. Hydrothermal aggregation induced crystallization: a facial route towards polycrystalline graphite quantum dots with blue photoluminescence. *CrystEngComm*, 2012, 14: 7149-7152.

13 Q. Feng, Q.Q. Cao, M. Li, F.C. Liu, N.J. Tang, Y.W. Du. Synthesis and photoluminescence of fluorinated graphene quantum dots. *Appl. Phys. Lett.*, 2013, 102: 013111.

14 M. Li, W.B. Wu, W.C. Ren, H.M. Cheng, N.J. Tang, W. Zhong, Y.W. Du. Synthesis and upconversion luminescence of N-doped graphene quantum dots. *Appl. Phys. Lett.*, 2013, 101: 013107.

15 J.H. Shen, Y.H. Zhu, X.L. Yang, J. Zong, J.M. Zhang, C.Z. Li. One-pot hydrothermal synthesis of graphene quantum dots surface-passivated by polyethylene glycol and their photoelectric conversion under near-infrared light. *New. J. Chem.*, 2012, 36: 97-101.

16 F. Yang, M.L. Zhao, B.Z. Zheng, D. Xiao, L. Wu, Y. Guo. Influence of pH on the fluorescence properties of graphene quantum dots using ozonation pre-oxide hydrothermal synthesis. J. *Mater. Chem.*, 2012, 22: 25471-25479.

17 S. Chen, J.W. Liu, M.L. Chen, X.W. Chen, J.H. Wang. Unusual emission transformation of graphene quantum dots induced by self-assembled aggregation. *Chem. Commun.*, 2012, 48: 7637-7639.

18 S.J. Zhu, J.H. Zhang, C.Y. Qiao, S.J. Tang, Y.F. Li, W.J. Yuan, B. Li, L. Tian, F. Liu, R. Hu, H.N. Gao, H.T. Wei, H. Zhang, H.C. Sun, B. Yang. Strongly green-photoluminescent graphene quantum dots for bioimaging applications. *Chem. Commun.*, 2011, 47: 6858-6860.

19 S.J. Zhu, J.H. Zhang, X. Liu, B. Li, X.F. Wang, S.J. Tang, Q.N. Meng, Y.F. Li, C. Shi, R. Hu, B. Yang. Graphene quantum dots with controllable surface oxidation, tunable fluorescence and up-conversion emission. *RSC Advan*ces, 2012, 2: 2717-2720.

20 Q. Liu, B.D. Guo, Z.Y. Rao, B.H. Zhang, J.R. Gong. Strong two-photon-induced fluorescence from photostable, biocompatible nitrogen-doped graphene quantum dots for cellular and deep-tissue imaging. *Nano Lett.*, 2013, dx.doi.org/10.1021/nl400368v.

21 W.J. Xie, Y.Y. Fu, H. Ma, M. Zhang, L.Z. Fan. Preparation of fluorescent graphene quantum dots as biological imaging marker for cells. *Acta Chim. Sinica*, 2012, 70: 2169-2172.

22 S.J. Zhu, J.H. Zhang, S.J. Tang, C.Y. Qiao, L. Wang, H.Y. Wang, X. Liu, B. Li, Y.F. Li, W.L. Yu, X.F. Wang, H.C. Sun, B. Yang. Surface chemistry routes to modulate the photoluminescence of graphene quantum dots: from fluorescence mechanism to up-conversion bioimaging applications. *Adv. Funct. Mater.*, 2012, 22: 4732-4740.

23 Z.M. Markovic, B.Z. Ristic, K.M. Arsikin, D.G. Klisic, L.M. Harhaji-Trajkovic, B.M. Todotovic-Markovic, D.P. Kepic, T.K. Kravic-Stevovic, S.P. Jovanovic, M.M. Milenkovic, D.D. Milivojevic, V.Z. Bumbasirevic, M.D. Dramicanin, V.S. Trajkovic. Graphene quantum dots as autophapy-inducing photodynamic agents. *Biomaterials*, 2012, 33: 7084-7092.

24 M. Zhang, L.L. Bai, W.H. Shang, W.J. Xie, H. Ma, Y.Y. Fu, D.C. Fang, H. Sun, L.Z. Fan, M. Han, C.M. Liu, S.H. Yang. Facile synthesis of water-soluble, highly fluorescent graphene quantum dots as a robust biological label for stem cells. *J. Mater. Chem.*, 2012, 22: 7461-7467.

25 L.M. Zhang, Y.D. Xing, N.Y. He, Y. Zhang, Z.X. Lu, J.P. Zhang, Z.J. Zhang. Preparation of graphene quantum dots for bioimaging application. *J. Nanosci. Nanotechnol.,* 2012, 12: 2924-2928.

26 J. Peng, W. Gao, B.K. Gupta, Z. Liu, R. Romero-Aburto, L.H. Ge, L. Song, L.B. Alemany, X.B. Zhan, G.H. Gao, S.A. Vithayathil, B.A. Kaipparettu, A.A. Marti, T. Hayashi, J.J. Zhu, P.M. Ajayan. Graphene quantum dots derived from carbon fibers. *Nano Lett.*, 2012, 12: 844-849.

27 H.J. Sun, L. Wu, N. Gao, J. S. Ren, X.G. Qu. Improvement of photoluminescence of graphene quantum dots with a biocompatible photochemical reduction pathway and its bioimaging application. *ACS Appl. Mater. Interfaces*, 2013, 5: 1174-1179.

28 Y.Q. Sun, S.Q. Wang, C. Li, P.H. Luo, L. Tao, Y. Wei, G. Q. Shi. Large scale preparation of graphene quantum dots from graphite with tunable fluorescence properties. *Phys. Chem. Chem. Phys.*, 2013, 15:9907-9913.

29 L. Deng, L. Liu, C.Z. Zhu, D. Li, S.J. Dong. Hybrid gold nanocube@ silica@graphene-quantum-dot superstructures: synthesis and specific cell surface protein imaging applications. *Chem. Commun.*, 2013, 49: 2503-2505.

30 M. Nurunnabi, Z. Khatun, G.R. Reeck, D.Y. Lee and Y.K. Lee. Near infra-red photoluminescence graphene nanoparticle greatly expands use in noninvasive biomedical imaging.*Chem. Commun*., 2013, 49: 5079-5081.

31 H.T. Li, X.D. He, Z.H. Kang, H. Huang, Y. Liu, J.L. Liu, S.Y. Lian, C.H. Tsang, X.B. Yang, S.T. Lee. Water-soluble fluorescence carbon

quantum dots and photocatalyst design. *Angew. Chem. Int. Ed.*, 2010, 49: 4430-4434.
32 H.P. Liu, T. Ye, C.D. Mao. Fluorescence carbon nanoparticles derived from candle soot. *Angew. Chem. Int. Ed.*, 2007, 46: 6473-6475.
33 S.K. Bhunia, A. Saha, A.R. Maity, S.C. Ray, N.R. Jana. Carbon nanoparticle-based fluorescence bioimaging probes. *Sci. Rep.*, 2013, 3: 1473.
34 X.M. Sun, Z. Liu, K. Welsher, J.T. Robinson, A. Goodwin, S. Zaric, H.J. Dai. Nano-graphene oxide for cellular imaging and drug delivery. *Nano Res.*, 2008, 1: 203-212.
35 Y.J. Jing, Y.H. Zhu, X.L. Yang, J.H. Shen, C.Z. Li. Ultrasound-triggered smart drug release from multifunctional core-shell capsules one-step fabricated by coaxial electrospray method. *Langmuir*, 2011, 27: 1175-1180.
36 X.J. Zhou, Y. Zhang, C. Wang, X.C.Wu, Y.Q. Yang, B. Zheng, H.X. Wu, S.W. Guo, J.Y. Zhang. Photo-fenton reaction of graphene oxide: a new strategy to prepare graphene quantum dots for DNA cleavage. *ACS Nano*, 2012, 6: 6592-6599.
37 H.L. Ren, C. Wang, J.L. Zhang, X.J. Zhou, D.F. Xu, J. Zheng, S.W. Guo, J.Y. Zhang. DNA cleavage system of nanosized graphene oxide sheets and copper ions. *ACS Nano*, 2010, 4: 7169-7174.
38 X. Chen, X.J. Zhou, T. Han, J.Y. Wu, J.Y. Zhang, S.W. Guo. Stabilization and induction of oligonucleotide i-motif structure via graphene quantum dots. *ACS Nano*, 2013, 7: 531-537.
39 H.M. Zhao, Y.Y. Chang, M. Liu, S. Gao, H.T. Yu, X. Quan. A universal immunosensing strategy based on regulation of the interaction between graphene and graphene quantum dots. *Chem. Commun*., 2013, 49: 234-236.
40 J.J. Liu, X.L. Zhang, Z.X. Cong, Z.T. Chen, H.H. Yang, G.N. Chen. Glutathione-functionalized graphene quantum dots as selective fluorescent probes for phosphate-containing metabolites. *Nanoscale*, 2013, 5: 1810-1815.
41 F. Jiang, D.Q. Chen, R. M.Li, Y.C. Wang, G.Q. Zhang, S.M. Li, J.P. Zheng, N.Y. Huang, Y. Gu, C.R. Wang, C.Y. Shu. Eco-friendly synthesis of size-controllable amine-functionalized graphene quantum dots with antimycoplasma properties. *Nanoscale,* 2013, 5: 1137-1142.

Copyright:(c) 2013 M.H Xu, et al. This is an open-access article distributed under the terms of the Creative Commons Attribution License, which permits unrestricted use, distribution, and reproduction in any medium, provided the original author and source are credited.